

WEATHERING PROCESSES IN BAKED SEDIMENTS AND THEIR EFFECTS ON ARCHAEO-MAGNETIC FIELD-INTENSITY MEASUREMENTS

M.F. BARBETTI *¹, M.W. McELHINNY, D.J. EDWARDS and P.W. SCHMIDT

*Research School of Earth Sciences, Australian National University, Canberra, A.C.T. (Australia) *²*

(Accepted for publication October 27, 1976)

Barbetti, M.F., McElhinny, M.W., Edwards, D.J. and Schmidt, P.W., 1977. Weathering processes in baked sediments and their effects on archaeomagnetic field-intensity measurements. *Phys. Earth Planet. Inter.*, 13: 346–354.

Thellier-type measurements of ancient field intensity on specimens of clay and other sediments, which were apparently well-baked and oxidised in ancient times, often fail to give consistent results over part or even most of the blocking-temperature spectrum. It is suggested that post-baking chemical alteration, or weathering, leading to the presence of hydrated Fe minerals, is a major cause of non-ideal behaviour in such material. The behaviour of hypothetical specimens containing either goethite or lepidocrocite can be predicted using simple models, and actual examples are given from two sites in southeastern Australia which show some similarities with the predicted model behaviour. The results of the Thellier measurements, after interpretation, agree closely with previously published results from the northern hemisphere for the period 4700–4200 yr. B.P. The presence of hydrated minerals may not be readily detected by methods other than the Thellier technique and, if so, would result in estimates of the ancient geomagnetic field strength that are systematically too low.

1. Introduction

Deposits of highly weathered sediment often contain a few percent by weight of various Fe-oxides and -oxyhydroxides which are progressively dehydrated and oxidised if the material is heated in air. This occurs in the sediment around burning logs, tree-stumps or man-made wooden structures, as well as fireplaces, ovens, kilns and in the prepared clay shapes which are fired to make pottery. With prolonged baking at more than 700°C in air all the Fe minerals are converted to haematite, which acquires a stable thermoremanent magnetization (TRM) as the material cools. The thermoremanence is both proportional and parallel to the applied magnetic field.

Material baked at a particular time and place therefore contains a record of the instantaneous geomagnetic

field intensity, and direction if it is found still in its original position. The Thellier and Thellier (1959) technique for measurement of ancient field intensity was originally developed for use with baked earth and pottery. Thellier-type measurements on experimentally-fired and well-preserved ancient material of this type, in which haematite is the predominant carrier of TRM, show an ideal linearity between original magnetization and laboratory thermoremanence over the entire blocking-temperature spectrum.

Frequently, however, Thellier-type measurements on apparently well-fired and oxidised sediment show deviations from linearity over some or even all parts of the blocking-temperature spectrum. Irreversible physico-chemical changes during laboratory heating, leading to an increase or decrease in TRM-bearing capacity at certain temperatures, are commonly the immediate cause of observed non-ideal behaviour. But why do such changes, so uncharacteristic of haematite, occur in ancient material which should have contained haematite as the sole magnetic mineral after baking in antiquity? Post-baking alteration, or weathering, is ob-

*¹ Now at Research Laboratory for Archaeology and the History of Art, 6 Keble Road, Oxford OX1 3QJ, Great Britain.

*² Address: Research School of Earth Sciences, Australian National University, P.O. Box 4, Canberra, A.C.T. 2600, Australia.

viously one process which can lead to the presence of unstable minerals in baked sediment.

In this paper we attempt to model, in a very simple way, the behaviour of specimens containing haematite and varying proportions of the hydrated Fe-oxides, goethite and lepidocrocite. We then compare the model predictions with some actual examples of non-ideal behaviour, observed in a study of baked sediments about 5000 yr. old from southeastern Australia. Certain similarities are evident between model and example, and we tentatively suggest a procedure for deducing the correct value of ancient field intensity for one characteristic type of non-ideal behaviour.

2. The Thellier method and the origin of the thermoremanence

Mössbauer studies (Hess and Perlman, 1974; Kostikas et al., 1974) of modern and ancient pottery, and the clay from which they were manufactured, have demonstrated that the haematite produced during firing has a broad grain-size distribution. This is consistent with the observation that TRM in baked sediment is usually distributed over a wide temperature range because, according to the theory of Néel (1949, 1955), the blocking temperature (T_B) is directly related to grain volume for a given material. The Mössbauer studies also indicate that the larger haematite grains are produced by grain growth, particularly during the high-temperature part of the firing. This phenomenon has not yet been apparent in laboratory studies of the TRM of baked sediment, but it may have some significance and we shall return to this point later.

The acquisition of TRM is a continuous process with cooling between the Curie temperature, T_C (675°C for haematite) and the final ambient temperature (about 20°C). If the grains are single-domained [$\gtrsim 0.15$ μm for haematite (Stacey, 1969)] and are dispersed so that there are no interactions between grains, the partial TRM (PTRM) acquired in any given T_B interval will be uniquely associated with that interval and completely independent of the state of magnetization of grains with T_B 's outside that interval. This leads to the *law of additivity of PTRM* (Thellier, 1951), which states that the observed total TRM is equal to the vector sum of all the PTRM's acquired separately over consecutive arbitrary temperature intervals.

We have made our ancient field intensity measurements using the Thellier and Thellier (1959) method, with the minor modification that the first heating and cooling at each temperature is performed in zero magnetic field [a procedure described by Nagata et al. (1963) and Coe (1967a)]. After the first heating, the remaining natural remanent magnetization (NRM) is measured. The specimen is then reheated to exactly the same temperature and cooled in a measured weak magnetic field to give it a laboratory PTRM in addition to the remaining partial NRM. If the specimen TRM-bearing capacity remains unchanged at all temperatures, and the law of additivity is obeyed, then the points on a graph of remaining partial NRM against acquired partial TRM for each temperature will define a straight line with negative slope equal to the ratio of ancient to laboratory magnetic fields (Nagata et al., 1963; Coe, 1967a). The plots are usually referred to as NRM–TRM diagrams.

In practice, for well-behaved specimens, the points will be slightly scattered about the ideal straight line because of experimental error, and the method of least-squares can be used to obtain an estimate of the true slope. Linearity of the points on an NRM–TRM diagram, which corresponds to a constant ratio of the partial NRM to PTRM associated with each member of a set of consecutive arbitrary temperature intervals, is a powerful argument for the absence of physical or chemical changes since the original cooling, and hence for the validity of the overall result.

Not infrequently, however, deviations from linearity are evident at low or high temperatures, and it is common practice to exclude these points and derive an estimate of the slope from the linear portion of the NRM–TRM diagram. This procedure is justifiable when linearity exists over a considerable temperature range so that the consistency argument can still be invoked, and a plausible explanation can be given for any non-linear region. Examples, of the latter are the effects of secondary components of magnetization (VRM) or PTRM acquired after the original firing (Thellier and Thellier, 1959; Coe, 1967b; Barbetti and McElhinny, 1976). Non-linear effects at high temperatures may arise if the material was originally baked below T_C (Schwarz and Christie, 1967; Bucha, 1971), or if physico-chemical changes (such as grain-size alteration or oxidation) occur during laboratory reheating (Nagata et al., 1963; Coe, 1967b; Bucha, 1971).

It is much more difficult to interpret NRM–TRM diagrams when they contain no significant linear segments. Various kinds of systematic curvature can arise if the material contains multidomain grains (Coe, 1967b) or interacting single-domain grains (Dunlop and West, 1969), so that the law of additivity does not apply. Other possible causes of systematic curvature are disparities in the original and laboratory cooling rates, changes in the demagnetizing field associated with the cutting of specimens, and non-linearity of PTRM with applied field (Coe, 1967b). Barbetti and McElhinny (1976) have suggested that systematic deviations from linearity may occur over most of the temperature range if the material has undergone weathering since the original firing, and is therefore contaminated with hydrated Fe minerals which are unstable to laboratory reheating.

Non-linear NRM–TRM diagrams with closely spaced points (corresponding to small temperature increments between successive heatings) generally show smooth trends and few, if any, are completely irregular. Attempts to use other techniques, such as the measurement of saturation magnetization or low-field susceptibility, as an aid for interpreting NRM–TRM diagrams have not been very successful, because of the variety of mechanisms which may lead to observable changes in the parameter being measured, and also because such techniques are often less sensitive indicators of changes than are the direct measurements of acquired PTRM performed as part of the Thellier method. These two factors lead us to suggest that it might be a useful approach to try and identify characteristic types of non-linear behaviour, some of which may be specific to a particular mineral or mechanism. If that process can be successfully modeled, then it should be possible to interpret at least some non-linear diagrams with confidence, and at the same time enlarge the range of ancient baked material on which reliable ancient field-intensity measurements can be made using the Thellier method.

3. A simple model for goethite and lepidocrocite contamination

The starting point is a hypothetical specimen of material which, immediately after cooling from above T_C , contains haematite as the sole magnetic mineral.

It is assumed that the resulting TRM is distributed evenly over the blocking-temperature spectrum from 0 to 600°C, and that no thermoremanence is associated with the temperature interval 600–675°C (because of a lack of haematite grains of the appropriate size). Some time later “weathering” commences, and a fraction of the TRM-bearing haematite is converted into one of the Fe-oxyhydroxides. For simplicity, it is assumed that equal fractions of the original PTRM are destroyed in each temperature interval, and that individual haematite grains are either unaltered or completely destroyed so that no redistribution with T_B occurs for the persistent TRM. The newly hydrated minerals carry negligible remanent magnetization. Alternatively, the oxyhydroxide mineral could simply be introduced from external surroundings, without any alteration of the TRM-bearing haematite.

Hypothetical NRM–TRM diagrams can be calculated when the hydrated mineral is either goethite (α -FeOOH) or lepidocrocite (γ -FeOOH), using published information on the magnetic properties and chemical transformations of these minerals (Hedley, 1968; Strangway et al., 1968; Strangway et al., 1969; Vlasov and Gornushkina, 1973), and assuming that the law of additivity of PTRM can be applied.

Two examples are shown in Fig. 1. In the first case, 25% of the final haematite is initially present in the specimen as goethite grains which remain passive until reverting to haematite grains between 300 and 375°C. In the second case, 0.5% of the final haematite is initially present as lepidocrocite grains which do not acquire a TRM, and dehydrate to form maghaemite between 225 and 300°C. The maghaemite grains are assumed to have randomly oriented moments on formation, and to have PTRM capacity evenly distributed between 0 and 600°C. Those grains with appropriate T_B 's then acquire a TRM (130 times stronger than for haematite) as they cool in the laboratory field. Above 375°C the maghaemite begins to revert to haematite, a process which is assumed to be half completed at 450°C, three-quarters completed at 525°C and completed at 600°C. In both cases the final haematite is assumed to have TRM capacity evenly distributed between 0 and 600°C.

The model predicts that the correct ratio between ancient and laboratory magnetic field can be found by calculating the slope from the low-temperature part of the NRM–TRM diagram, before chemical

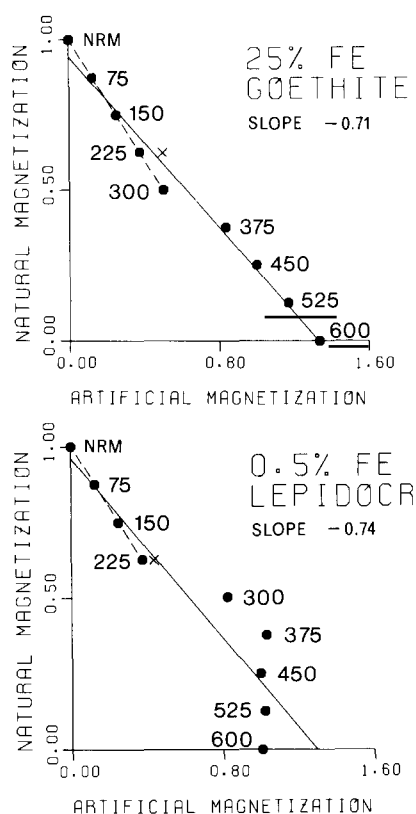


Fig. 1. Hypothetical NRM-TRM diagrams for specimens containing hydrated Fe oxide minerals, when the "original" and "laboratory" magnetic fields are equal. Calculated magnetic moments are normalized, with the total NRM taken as unity. Numbers near the points indicate the "heating" temperatures in °C, with repeated PTRM's from 225°C, performed after laboratory "heatings" have progressed to 525°C, shown by crosses. Least-squares fitted lines, including all points (continuous lines with incorrect slopes) and low temperature points only (dashed lines with slopes of -1) are shown. Details of the calculations are given in the text.

transformation of the Fe-oxyhydroxide minerals occurs. This result is independent of the particular grain-size distributions chosen and should have general application whenever interactions between grains are negligible and the T_B 's of surviving TRM-bearing grains have not changed since the original firing.

4. An example of weathering effects

4.1. The sites

In 1971 and 1972 a total of eight sites were found in a section of an ancient point-bar deposit, exposed by modern river-bank erosion of the Murray River in southeastern Australia, at latitude 35.6°S and longitude 144.5°E. Pellets of charcoal and lumps of baked sediment, ranging from 1 to about 15 cm across, were found interspersed with soft unbaked sediment, and are thought to result from the burning of logs, tree-stumps or roots. Unoriented samples of hard, brick-red material were collected from the two sites (MR7 and MR9) for which results are reported here.

4.2. Ages

Radiocarbon age determinations have been made on charcoal from the eight sites, and details have been published by Barbetti and Polach (1973) and Polach et al. (1976). Ages for MR7 and MR9 are given in Table I.

The eight burnt zones were sealed beneath several metres of gently-dipping sediments, and are therefore considered to be contemporary with sediment deposition at the edge of the growing point-bar. With this

TABLE I
 ^{14}C ages of sites

Site	Laboratory No.	Conventional ^{14}C age (yr. B.P.)	True age 68% confidence (yr. B.P.)	Limits at 95% confidence (yr. B.P.)
MR7	ANU-699	4550 ± 60	5180-5445	5010-5560
MR9	ANU-1084	4580 ± 250	5010-5625	4645-5880

Conventional radiocarbon ages (yr. B.P.) are calculated using 5568-yr. half-life, with the uncertainty arising from counting statistics given at one standard error (68%-confidence level); details are given in Polach et al. (1976). The calibration procedure of Clark (1975) has been used to place confidence intervals on the true age in years B.P.

assumption, analysis of the calibrated radiocarbon ages and the positions of the sites along the point-bar indicates a constant rate of extension $\sim 0.09 \text{ myr.}^{-1}$ between 7000 yr. B.P. and the present-day. The horizontal separation of 39 m between MR7 and MR9 therefore suggests that the latter site might be ~ 400 yr. younger, and this is consistent with the calibrated radiocarbon ages at the 95%-confidence level.

4.3. Ancient field intensity measurements

Cylindrical specimens (28 mm diameter, 28 mm long) were cut from the unoriented lumps of baked sediment, and their total NRM was measured using a Digico spinner magnetometer (Molyneux, 1971). Good agreement in direction was found in all cases where more than one specimen was obtained from a single lump. Specimens for Thellier-type ancient field-intensity measurements were chosen so that a representative range of colours and specific magnetizations would be included for each site. The double-heatings were performed using specially designed furnaces (Barbetti, 1973) in an automatically controlled field-free space described by McElhinny et al. (1971). A heating time of 1 h was used, allowing approximately 20 min soaking after stabilization at the preselected temperature. The second heating and cooling at each temperature was performed in a laboratory field of $59.3 \mu\text{T}$ (equivalent to 0.593 Oe).

The NRM directions were found to be stable, with changes of less than 10° occurring for thermal demagnetization up to 600°C , a temperature at which only about 2% of the original magnetization remained. This indicates that none of the baked material studied had moved significantly during the original cooling, and that the dispersion of the lumps within the sediment must have occurred after cooling. The fact that even the softer less well-baked material possessed a stable magnetization up to 600°C suggests that the harder brick-red material was originally baked well in excess of 600°C , which is consistent with everyday experience that temperatures around $1,000^\circ\text{C}$ are required to produce the latter type of material.

NRM–TRM diagrams are illustrated in Fig. 2 for the twelve specimens studied from sites MR7 and MR9. Details of the slope analysis are given in Table II. The first ten specimens display an enhanced PTRM capacity between 300 and 540°C , which is very similar to

the predicted model behaviour for a specimen containing a very small amount ($\leq 2\%$) of lepidocrocite. The remaining two specimens, MR9-A1 and -D1, show a continuous curvature of a different nature which is not adequately predicted by either model, but is similar to the behaviour reported by Barbetti and McElhinny (1976) and frequently observed by us (unpublished data) in specimens of baked earth from ancient fireplaces exposed in open country in southeastern Australia.

Using the models described earlier, we have interpreted and illustrated the NRM–TRM diagrams in the following way. For the first ten specimens we have calculated a least-squares slope using only data at 120°C (where available), 180°C , 240°C and 600°C ; except, that is, for the two specimens (MR7-A1 and -B1) for which a well-defined slope could be obtained without including the measurements at 600°C . Strictly speaking, we should not have used any of the data at 600°C , because, according to our model, the TRM capacity will have increased by up to 2%, depending on the amount of lepidocrocite initially present during laboratory heating. Increases of about 4 and 6% (respectively) are suggested by the NRM–TRM diagrams for MR7-A1 and -B1, and it is possible therefore that the calculated slopes for the other eight specimens might be as much as about 5% too low. For the last two specimens (MR9-A1 and -D1) the calculated slopes, using data at 180, 240 and 300°C , are broadly consistent with results from the other specimens but, because we do not yet have a quantitative predictive model for the type of non-ideal behaviour displayed, these results have not been included in the calculation of the site mean (Table II).

4.4. Discussion

It can be seen from Table II that, although the accepted slopes (calculated after interpretation) are not noticeably more tightly grouped than slopes calculated using data at all temperatures, a significant decrease has occurred in the associated standard errors. This is in accord with the model prediction that data below 300°C and, to a lesser extent, data at 600°C should exhibit linearity.

We believe that the accepted slopes (Table II) are the best estimates that can be derived from the available data. All the specimens have been reheated in the earth's

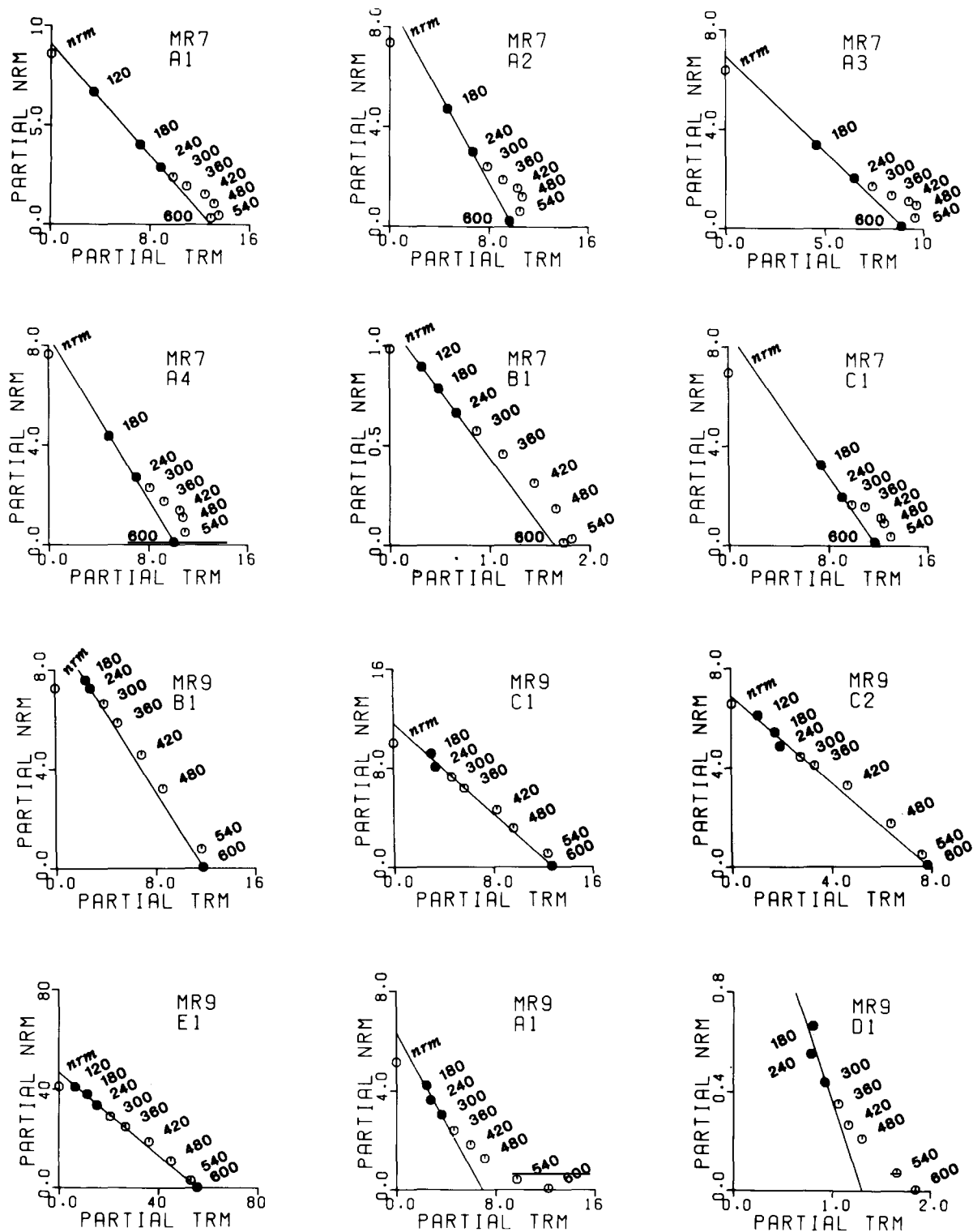


Fig. 2. NRM-TRM diagrams for the twelve specimens studied from sites MR7 and MR9. Specific magnetizations are plotted, in units of $10^{-4} \text{ Am}^2 \text{ kg}^{-1}$. Numbers near the points give the double-heating temperatures in °C. Least-squares fitted lines were obtained using selected data (solid symbols).

TABLE II
Slopes of NRM–TRM diagrams

Specimen	Least-squares analysis performed using data at				Site mean
	all temperatures except NRM	180, 240, 300°C	120, 180, 240, 600°C	180, 240, 600°C	
MR7-A1	-0.59 ± 0.04				-0.71 ± 0.002
MR7-A2	-0.62 ± 0.10			-0.89 ± 0.03	
MR7-A3	-0.53 ± 0.09			-0.76 ± 0.03	-0.76
MR7-A4	-0.59 ± 0.09			-0.82 ± 0.03	±0.07 (standard deviation)
MR7-B1	-0.56 ± 0.03				-0.67 ± 0.008
MR7-C1	-0.47 ± 0.09			-0.72 ± 0.03	±0.03 (standard error)
MR9-B1	-0.77 ± 0.03			-0.81 ± 0.003	
MR9-C1	-0.86 ± 0.04			-0.91 ± 0.07	
MR9-C2	-0.83 ± 0.03		-0.87 ± 0.05		-0.86
MR9-E1	-0.81 ± 0.02		-0.84 ± 0.02		±0.04 (standard deviation)
MR9-A1	-0.41 ± 0.05	-0.91 ± 0.25			±0.02 (standard error)
MR9-D1	-0.57 ± 0.07	-1.19 ± 0.88			

Standard errors are quoted to the slope. Values to the right, obtained using data at selected temperatures (as illustrated in Fig. 2), have been used to calculate the site mean ratios of ancient geomagnetic and laboratory magnetic field intensity; slopes for MR9-A1 and -D1 have very large standard errors and were not included.

field to temperatures of 420 and 480°C and it has been confirmed that the greatly increased TRM capacity, ascribed to the temporary presence of maghaemite during the first heatings, does not reappear in the first eight specimens after they have been heated at 600°C. These repeat measurements do not, however, allow a more precise slope to be calculated, because of the presence of small amounts of additional haematite formed by chemical transformation.

The least-squares slopes calculated for specimens MR9-A1 and -D1 using data at all temperatures are low in comparison with slopes for the other specimens and the site mean. This is in accord with our experience (unpublished data) that systematically low values are obtained from specimens displaying this type of convex-downwards curvature. In a detailed study of specimens displaying this type of alteration, Barbetti and McElhinny (1976) found, as in the present study, no significant difference between the first PTRM's and repeat values at the same temperatures, performed *after* laboratory heatings had been done at higher temperatures, and that convex curvature was not observed

in Thellier-type measurements of a *laboratory* TRM in the same specimens. This type of behaviour may be due to the presence of a hydrated mineral or minerals which undergo chemical transformation at about 100°C. It is also possible that weathering may produce altered rims on some haematite grains, with the result that grain enlargement would occur with dehydration during laboratory heating. The origin of this type of behaviour must remain somewhat speculative at the moment, even though we know that it always leads to systematically low estimates of ancient field intensity if data at all temperatures are included in the slope calculation.

Table III gives the site mean values for the ancient field intensity and the corresponding values for the virtual axial dipole moment (VADM), calculated on the assumption that the measured field is due to a geocentric dipole aligned with the earth's rotation axis. It is not possible to calculate a virtual dipole moment in the normal way, because the palaeo-inclination is not known for these sites, and a difference of about 23% in the calculated dipole moment would occur if

TABLE III

Dipole moments

Site	Ancient field intensity (μT)	Virtual axial dipole moment (10^{22} Am^2)
MR7	45 ± 2	8.2 ± 0.3
MR9	51 ± 1	9.3 ± 0.2

Standard errors are quoted. Dipole moments are calculated assuming a geocentric *axial* source (inclination -55°), and the uncertainty does not include an allowance for possible error arising from this assumption.

the actual palaeo-inclination differed by 20°C from the assumed axial dipole inclination of -55° . The VADM values in Table III, the first data for this period from the southern hemisphere, are however in close agreement with mean value of $(8.9 \pm 1.0) \cdot 10^{22} \text{ Am}^2$ for sites in Japan and the U.S.S.R. for the period 2750–2250 yr. B.C. (Smith, 1970).

5. Conclusions

(1) That significant post firing chemical alteration or weathering is probably common in baked clay and sediment which has not been preserved in a dry environment.

(2) Weathering may produce a variety of hydrated Fe minerals, depending on the microchemical conditions.

(3) That very small amounts of these hydrated minerals can produce large deviations from linearity during Thellier-type measurements of ancient field intensity.

(4) When the dominant hydrated mineral happens to be lepidocrocite ($\gamma\text{-FeOOH}$), the result is a characteristic NRM–TRM diagram which can be interpreted with reasonable confidence using a simple model to explain the observed behaviour.

(5) The presence of hydrated minerals other than lepidocrocite results in non-linear NRM–TRM diagrams which are not yet fully understood, but nevertheless are known to yield systematically low estimates of ancient field intensity because of increases in TRM capacity during laboratory heating.

(6) The presence of hydrated minerals may not be readily detected with methods, other than the Thellier

techniques, which rely on a single heating to T_C . The derived estimates of ancient field intensity will be systematically too low.

(7) The VADM values reported here agree closely with previously reported values from northern-hemisphere sites with the same (conventional) radiocarbon ages.

Acknowledgements

We thank J. Bowler of the Department of Biogeography and Geomorphology, Australian National University for suggesting these sites to us, and J. Urquhart (formerly of the same Department) for his help with sample collection.

References

- Barbetti, M., 1973. A furnace for archaeomagnetic and palaeomagnetic experiments. Research School of Earth Sciences, Australian National University, Canberra, A.C.T., Publ. No. 997.
- Barbetti, M.F. and McElhinny, M.W., 1976. The Lake Mungo geomagnetic excursion. *Philos. Trans. R. Soc. London*, 281: 515–542.
- Barbetti, M. and Polach, H., 1973. ANU radiocarbon data list, V. *Radiocarbon*, 15: 241–251.
- Bucha, V., 1971. Archaeomagnetic dating. In: H.N. Michael and E.K. Ralph (Editors), *Dating Techniques for the Archaeologist*. MIT Press, Cambridge, Mass., pp. 57–115.
- Clark, R.M., 1975. A calibration curve for radiocarbon dates. *Antiquity*, 49: 251–266.
- Coe, R.S., 1967a. Palaeointensities of the Earth's magnetic field determined from Tertiary and Quaternary rocks. *J. Geophys. Res.*, 72: 3247–3262.
- Coe, R.S., 1967b. The determination of palaeointensities of the Earth's magnetic field with emphasis on mechanisms which could cause non-ideal behaviour in Thellier's method. *J. Geomagn. Geoelectr.*, 19: 157–179.
- Dunlop, D.J. and West, G.F., 1969. An experimental evaluation of single domain theories. *Rev. Geophys.*, 7: 709–757.
- Hedley, I.G., 1968. Chemical remanent magnetization of the FeOOH, Fe₂O₃ system. *Phys. Earth Planet. Inter.*, 1: 103–121.
- Hess, J. and Perlman, I., 1974. Mössbauer spectra of iron in ceramics and their relation to pottery colours. *Archaeometry*, 16: 137–152.
- Kostikas, A., Simopoulos, A. and Gangas, N.H., 1974. Mössbauer studies of ancient pottery. *J. Phys. (Paris), (Colloq. C1)*, 35: C1-107–C1-115.

- McElhinny, M.W., Luck, G.R. and Edwards, D., 1971. A large volume magnetic field free space for thermal demagnetization and other experiments in palaeomagnetism. *Pure Appl. Geophys.*, 90: 126–130.
- Molyneux, L., 1971. A complete resist magnetometer for measuring the remanent magnetization of rocks. *Geophys. J.R. Astron. Soc.*, 24: 429–433.
- Nagata, T., Arai, Y. and Momose, K., 1963. Secular variation of the total geomagnetic force during the last 5000 years. *J. Geophys. Res.*, 68: 5277–5281.
- Néel, L., 1949. Théorie de trainage magnétique des ferromagnétiques en grains fins avec application aux terres cuites. *Ann. Géophys.*, 5: 99–136.
- Néel, L., 1955. Some theoretical aspects of rock magnetism. *Philos. Mag., Suppl. Adv. Phys.*, 4: 191–243.
- Polach, H.A., Head, M.J., Gower, J.D. and Quiggin, P.H., 1976. ANU radiocarbon date list, VI. Radiocarbon (to be published).
- Schwarz, E.J. and Christie, K.W., 1967. Original remanent magnetization of Ontario potsherds. *J. Geophys. Res.*, 72: 3263–3269.
- Smith, P.J., 1970. Intensity of the ancient geomagnetic field: A summary of conclusions. In: S.K. Runcorn (Editor), *Palaeogeophysics*, Academic Press, London, pp. 79–90.
- Stacey, F.D., 1969. *Physics of the Earth*. Wiley, New York, N.Y., 195 pp.
- Strangway, D.W., Honea, R.M., McMahon, B.E. and Larson, E.E., 1968. The magnetic properties of naturally occurring goethite. *Geophys. J.R. Astron. Soc.*, 15: 345–359.
- Strangway, D.W., McMahon, B.E. and Bischoff, J.L., 1969. Magnetic properties of minerals from the Red Sea thermal brines. In: E.T. Degens and D.A. Ross (Editors), *Hot Brines and Recent Heavy Metal Deposits in the Red Sea*, Springer, New York, N.Y., pp. 460–473.
- Thellier, E., 1951. Propriétés magnétiques des terres cuites et des roches. Rapport au colloque sur le ferromagnétisme et l'antiferromagnétisme, Grenoble, 1950. *J. Phys. (Paris)*, 12: 205–218.
- Thellier, E. and Thellier, O., 1959. Sur l'intensité du champ magnétique terrestre dans le passé historique et géologique. *Ann. Géophys.*, 15: 285–376.
- Vlasov, A.Ya. and Gornushkina, N.A., 1973. Chemical remanent magnetization during the lepidocrocite–maghemite–hematite temperature transformation. *Izv. Acad. Sci. U.S.S.R., Phys. Solid Earth*, 2: 110–115 (translation of *Izv. Akad. Nauk S.S.S.R., Fiz. Zemli*, 2: 70–79).